Biosensors and Bioelectronics 25 (2009) 864–869

Contents lists available at ScienceDirect

Biosensors and Bioelectronics

journal homepage: www.elsevier.com/locate/bios

Fiber optic SPR biosensing of DNA hybridization and DNA–protein interactions

Jeroen Pollet[a], Filip Delport[a], Kris P.F. Janssen[a], Karolien Jans[b], Guido Maes[c], Helge Pfeiffer[d], Martine Wevers[d], Jeroen Lammertyn[a,*]

[a] BIOSYST-MeBioS, Katholieke Universiteit Leuven, Willem de Croylaan 42, B-3001 Leuven, Belgium
[b] Interuniversity Microelectronics Center (IMEC), Kapeldreef 75, B-3001 Leuven, Belgium
[c] Quantum Chemistry and Physical Chemistry Section, Katholieke Universiteit Leuven, Celestijnenlaan 200F, B-3001 Leuven, Belgium
[d] Mechanical Metallurgy Section, Katholieke Universiteit Leuven, Kasteelpark Arenberg 44, B-3001 Leuven, Belgium

ARTICLE INFO

Article history:
Received 4 June 2009
Received in revised form 26 August 2009
Accepted 28 August 2009
Available online 3 September 2009

Keywords:
DNA hybridization
Aptamers
Surface plasmon resonance
Fiber optic biosensor
DNA–protein interactions

ABSTRACT

In this paper we present a fiber optic surface plasmon resonance (SPR) sensor as a reusable, cost-effective and label free biosensor for measuring DNA hybridization and DNA–protein interactions. This is the first paper that combines the concept of a fiber-based SPR system with DNA aptamer bioreceptors. The fibers were sputtered with a 50 nm gold layer which was then covered with a protein repulsive self-assembled monolayer of mixed polyethylene glycol (PEG). Streptavidin was attached to the PEG's carboxyl groups to serve as a versatile binding element for biotinylated ssDNA. The ssDNA coated SPR fibers were first evaluated as a nucleic acid biosensor through a DNA–DNA hybridization assay for a random 37-mer ssDNA. This single stranded DNA showed a 15 nucleotides overlap with the receptor ssDNA on the SPR fiber. A linear calibration curve was observed in 0.5–5 μM range. A negative control test did not reveal any significant non-specific binding, and the biosensor was easily regenerated. In a second assay the fiber optic SPR biosensor was functionalized with ssDNA aptamers against human immunoglobulin E. Limits of detection (2 nM) and quantification (6 nM) in the low nanomolar range were observed. The presented biosensor was not only useful for DNA and protein quantification purposes, but also to reveal the binding kinetics occurring at the sensor surface. The dissociation constant between aptamer and hIgE was equal to 30.9 ± 2.9 nM. The observed kinetics fully comply with most data from the literature and were also confirmed by own control measurements.

1. Introduction

Surface plasmon resonance (SPR) is probably one of the most suitable methods for real time detection and monitoring of biological binding reactions (Yang et al., 2007). The technique offers valuable information for many industrial and medical applications. Nevertheless, SPR is rarely used outside research centers, because most commercially available systems are expensive and require specialized staff. In the search for more convenient and cost-effective SPR sensors, Jorgenson and Yee (1993) replaced the traditional prism-based systems by a fiber optic design. The fiber-optic SPR probes are useful for remote sensing, continuous analysis and in situ monitoring. Numerous versions have been introduced in an attempt to optimize the sensitivity of the sensor platform (Masson et al., 2006; Mitsushio and Higo, 2004; Slavik et al., 1999). Nevertheless, only a few different biosensing applications were reported. Based on literature (Myszka, 1999; Shankaran and Miura, 2007) and our personal experience with the SPR, we believe that part of the key towards better fiber optic SPR biosensors is controlling the chemical interactions on the sensor surface. In this paper we combined the use of mixed polyethyleen glycol (PEG) chains as protein repulsive ground layer and single stranded DNA (ssDNA) as bio-recognition elements on the SPR fibers. ssDNA is not only used as a receptor for complementary stands in a classical hybridization assay, it can also serve as an aptamer. Aptamers are nucleic acids which have the potential to bind to specific target molecules with high affinity. These oligonucleotides are usually selected in vitro through the systematic evolution of ligands by the exponential enrichment (SELEX) process. Similar to antibodies, aptamers are highly selective for their target over other molecules. Their most pronounced advantages over antibodies are their stability to biodegradation and their low production cost (Jayasena, 1999). Over the years aptamers have gained interest as reliable bioreceptors against various target molecules in biological samples leading to interesting medical applications (Mayer, 2009; Song et al., 2008).

* Corresponding author. Tel.: +32 16321459; fax: +32 16322955.
E-mail addresses: jeroen.pollet@biw.kuleuven.be (J. Pollet), filip.delport@biw.kuleuven.be (F. Delport), Kris.Janssen@biw.kuleuven.be (K.P.F. Janssen), karolien.jans@imec.be (K. Jans), guido.maes@chem.kuleuven.be (G. Maes), helge.pfeiffer@mtm.kuleuven.be (H. Pfeiffer), martine.wevers@mtm.kuleuven.be (M. Wevers), jeroen.lammertyn@biw.kuleuven.be (J. Lammertyn).

0956-5663/$ – see front matter © 2009 Elsevier B.V. All rights reserved.
doi:10.1016/j.bios.2009.08.045

This is the first report on fiber optic SPR using DNA aptamers as bioreceptors. Our objective is to utilize the high stability of the ssDNA to develop reusable and cost-effective biosensors for DNA and protein detection. A mixed PEG ground layer will be used to optimize the biosensor selectivity. In a DNA–DNA hybridization assay the excellent sensitivity and selectivity of our low cost biosensor will be demonstrated. The principle will be further challenged by coating our fibers with DNA–aptamers against human Immunoglobulin E (hIgE), selected by Wiegand et al. (1996). This target protein plays an important role in many allergic reactions. hIgE aptamers have been successfully implemented in different transducer systems for developing label free biosensors (de-los-Santos-Alvarez et al., 2008), and many of these reports confirm that the aptamer-based sensors are a valuable alternative to immunosensors. However, we noticed a significant variance in the published results on the binding kinetics of hIgE and hIgE aptamers on different biosensor platforms (Gong et al., 2007; Kim et al., 2009; Wang et al., 2008).

The results obtained by the new fiber-based SPR platform will be validated and evaluated with a Biacore 3000 as a SPR reference system.

2. Materials and methods

2.1. Preparation of the fiber optic SPR probes

The optical probes (Fig. 1) were constructed with TEQS^{TM} multimode fibers (Thorlabs, Munich, Germany) with a diameter of 400 μm and a numerical aperture of 0.39. The fibers were cut in pieces of 3 cm and fixed with epoxy-glue inside a syringe needle. The plastic cap of the needle was adapted for perfect fitting onto the backside of an SMA connector (Avantes BV, Eerbeek, The Netherlands). A 1 cm SPR-sensitive zone was constructed at the side of the fiber tip. Hereto, the polymer cladding was carefully removed with acetone. Afterwards, the stripped part of the fibers was cleaned in 30:70 (v/v) solution of 30% hydrogen peroxide and concentrated sulphuric acid. The cleaned fibers were coated in a gold sputter coater (Balzers, Liechtenstein) for 1 min to deposit a 50 nm gold layer. The metal layers at the end of the tip acted as a mirror and reflected the light back to the spectrometer. Scanning electron microscopy (XL 30 ESEM, Philips Electronics N.V. Eindhoven, The Netherlands) was used to inspect irregularities on the fiber surface. The surface morphology of the deposited gold films was visualized and analyzed with atomic force microscopy (Multimode V., Veeco Instruments, Breda, The Netherlands). A smooth surface is preferred in order to have a uniform surface available for coupling ssDNA bioreceptors. The root mean square average of the surface profile (R_q) was estimated to be 3.659 nm.

2.2. Apparatus and system setup

The replaceable and interchangeable sensing probes are affixed onto the end of a bifurcated optical fiber which guides white light from a LS-1 tungsten halogen light source (Ocean Optics, Dunedin, USA) into the sensor probes. The light reflected at the gold tip of the probe is collected by a spectrophotometer, with a detection range from 350 to 1100 nm (USB4000, Ocean Optics, Dunedin, USA) (Fig. 1) and results in the typical spectral resonance SPR-dip. The presented SPR sensor measures wavelength modulations of the SPR-dip. The distribution of the angles at which the light wave is incident onto the gold layer is presumed to be constant. The strength of the coupling between the incident wave and surface plasmon is observed at multiple wavelengths and the wavelength yielding the strongest coupling, the 'resonance wavelength' is used as the sensor output (Homola and Piliarik, 2006). A binding event on the gold layer disturbs the surface plasmons, changes the resonance conditions and hence induces the resonance wavelength to shift allowing the surface chemistry to be monitored in real time. The fiber probe is attached to a pre-programmed computer-controlled robot (Colinbus, Hulshout, Belgium) to integrate it into a fully automated system. The robot was programmed to position the SPR fiber probe both in 96-well microplates and standard 1 ml glass vials and allowed repeatable, fast and easy immobilization procedures and measurements.

In contrast to our setup, the Biacore 3000 SPR platform measures the resonance phenomenon by angle modulation. The system makes use of a single wavelength light source which is focused by a glass prism on a 4 channel microfluidic chip.

2.3. Reagents

All buffer reagents were supplied by Sigma–Aldrich (Bornem, Belgium). Every solution was prepared with deionized water purified with a Milli-Q Plus system (Millipore, Marlborough, MA, USA). Carboxylic acid-capped hexa(ethylene glycol) undecanethiol (SHC11(PEO)6COOH) was obtained from SensoPath Technologies, and (1-mercapto-11-undecyl)tri(ethylene glycol) (SHC11(PEO)3OH) was synthesized as described previously (Palegrosdemange et al., 1991). The 1 mM mixed polyethylene glycol (PEG) layer, used in the experiments, consisted of 5% carboxylic acid-capped PEG undecanethiol and 95% hydroxyl PEG undecanethiol (Jans et al., 2008). 1-Ethyl-3-[3-dimethyl aminopropyl]carbodiimide hydrochloride (EDC) was obtained from Pierce Biotechnology (Rockford, USA). Streptavidin and Human IgG was supplied by Sigma–Aldrich (Bornem, Belgium). Human myeloma IgE kappa (1.5 mg/ml) was supplied by Athens Research and Technology (Georgia, USA).

All ssDNA was synthesized, purified and biotin-labeled by Eurogentec (Luik, Belgium).

The aptamers were extended with 24 thymidine bases at the 3′ biotin binding site to give the aptamer maximum flexibility for binding with IgE proteins. The full sequence of the aptamer was 5′-GGGGCACGTTTATCCGTCCCTCCTAGTGGCGTGCCCC T_{24}-3′. For practical reasons we used the same DNA sequence, without the poly T extension, in the hybridization assay. In the latter assay this 37-mer DNA is only used as a random complementary target and not as an aptamer. The biotinylated DNA used to capture the 37-mer DNA was sequenced as 5′-GGATAAACGTGCCCCTTTTTTTTTT-3′. The thymidine was again added for more flexibility. The complementary target oligonucleotide had a 15 base pairs overlap from the 5′ side. A shuffled version of the 37-mer DNA was used as the non-complementary DNA sequence to evaluate non-specific adsorption, 5′-TTCCCCGGCCTGGGCTCG GGACCCACTCGTGCTGTCC3′.

2.4. Surface chemistry

In a first step a self-assembled monolayer of 5% carboxylic acid-capped hexa(ethylene glycol) undecanethiol and 95% (1-mercapto-11-undecyl)tri(ethylene glycol) was used as a prime layer. This layer significantly reduces non-specific adsorption due to its high hydrophilic character and maximum chain flexibility. The presence of tightly bound water molecules around the PEG molecules prevents uncontrolled protein absorption. Steric repulsion, resulting from the compression of PEG chains, also minimizes non-specific surface interactions (Shankaran and Miura, 2007). On this layer, streptavidin (0.02 mg/ml) was immobilized trough the zero length linker EDC (0.5 mM) in a 100 mM 2-(*N*-morpholino) ethanesulfonic acid (MES) buffer. The biotinylated ssDNA aptamers were coupled to the active sites of the latter protein using a buffer containing 10 mM Tris–HCl, 300 mM NaCl, 1 mM EDTA at pH 7.5. DNA hybridization experiments were car-

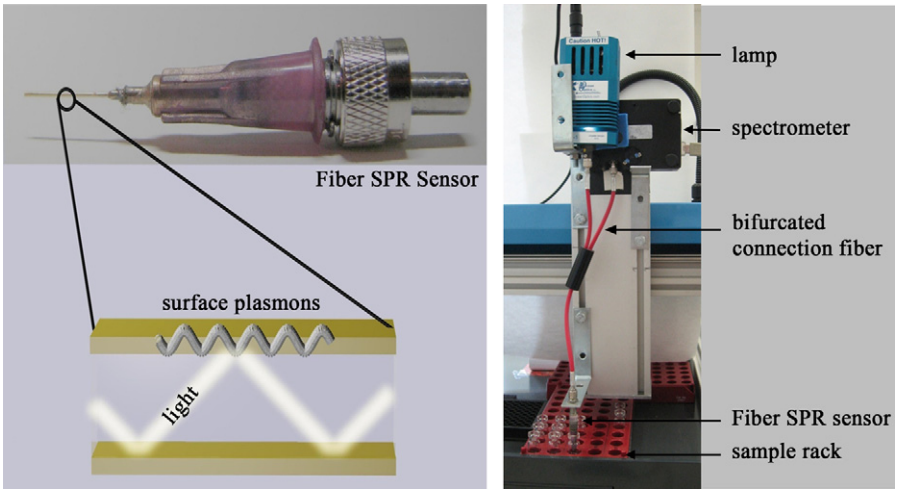

Fig. 1. The SPR system. (A) The fiber surface plasmon resonance sensor and a schematic interpretation of the sensor tip intersection. (B) The system setup mounted on a computer-controlled positioning robot.

ried out in a concentrated NaCl (1 M) TRIS buffer (pH 7.5). The regeneration of the DNA-coated surface was achieved with 2 mM HCl, which denatures the hybridized DNA. The aptamer–protein (hIgE) binding reaction was performed in a TGK buffer solution (25 mM Tris(hydroxyamino)methane, 192 mM glycine, 5 mM K_2HPO_4) adjusted to pH 8.4. The buffer was selected for optimal binding kinetics between hIgE aptamer and hIgE (Buchanan et al., 2003). The binding kinetics were studied on a MDQ capillary electrophoresis system (Beckman Coulter, Fullerton, USA) with a 488 nm argon laser and a Biacore 3000 system (Biacore AB, Uppsala, Sweden).

2.5. Data processing

Data were recorded with Spectrasuite (Ocean Optics, Dunedin, USA) and further processed using Matlab software (Mathworks, Natick, USA). Each SPR spectrum is the ratio of the 'spectrum of the sample' and the 'air-based reference spectrum'. The raw data were filtered with a Savitsky–Golay filter. The resonance wavelength was finally calculated using the Minimum Hunt Method (Grunwald and Holst, 2004). In this method a second order polynomial is fit to the SPR-dip to determine the local minimum. As a result of the different data process steps, the impact of modal noise in the multimode fibers on the signal was controllable. In the resulting sensorgrams the SPR wavelength shift (nm) is plotted versus time. The data of the different wash steps are cut out, because of the distinctly different refraction index. This allows zooming in more on the kinetic data. The wash steps are indicated by an asterisk symbol in the time resolved figures. The statistical analysis of the binding kinetics on the SPR fiber was done based on a 1:1 Langmuir model using Prism (Graphpad Software, San Diego, USA). The evaluation of the binding kinetics in the capillary electrophoresis unit was done according to the protocols described by Berezovski et al. (2006). BIA evaluation 3.1 software (Biacore AB, Uppsala, Sweden) was used for processing all data from the Biacore 3000.

3. Results and discussion

3.1. Fiber evaluation

The surface plasmon resonance phenomenon is very sensitive to changes of the refraction index near the gold surface. Regardless of any surface binding event, the increase of refraction index (mass) will induce a red shift of the dip in the SPR reflection signal towards longer wavelengths (Fig. 2A). We first validated the sensors by measuring a set of sucrose in water solutions with concentrations ranging from 0 to 7% (Fig. 2B). Each sample was measured three times to demonstrate the reproducibility of the system. Between two subsequent measurements the SPR probe was rinsed with water, which is reflected in Fig. 2B by the sharp decreases in signal intensity between two subsequent sucrose measurements. The average coefficient of variation was 0.3%. In order to evaluate and calibrate the sensor probes faster, different alcohol solutions were used instead of sucrose solutions. The known refraction index units of the alcohols were linked to the sensors SPR wavelength shift (Fig. 2C and D) to determine the SPR sensor sensitivity. As expected from data in the literature, a non-linear relation was observed in the refraction index range between 1.33 and 1.42 refraction index units (RIU) (Obando and Booksh, 1999). However, for the first part of the calibration curve (from 1.33 to 1.37 RIU), the response of the surface plasmon shift did show a linear relation with the refraction index (Fig. 2D). The variation on slope of different fibers was limited to 5%. The average refraction index resolution of the probes is estimated to be 2.10^{-4} RIU, which is in line with previous data of other authors (Grunwald and Holst, 2004). From these results it was concluded that the fiber sensitivity is sufficiently high for biosensing purposes.

3.2. DNA immobilization

The formation of a self-assembling monolayer and the ssDNA immobilization procedure was monitored in real time using the SPR fiber. In a first step, a mixed self-assembled monolayer of hydroxyl/carboxyl mercapto-PEG was formed on the gold sensor surface by an overnight incubation step. The carboxyl termini of the mixed monolayer were activated by EDC to immobilize streptavidin. Afterwards the sensor surface was washed with NaOH (50 mM) in NaCl (1 M) to remove any unbound streptavidin. Block A of Figs. 3 and 5 show the sensor response induced by this event. The net SPR wavelength shift, after the washing procedure, was 4.5 ± 1.0 nm in MES-buffer, and varied slightly in between individual fibers and incubation time. When the protocol was executed on a Biacore 3000 system a streptavidin immobilization degree of 1289.2 ± 106.8 RU or 1289.2 ± 106.8 pg/mm^2 was observed. It is assumed that the density of streptavidin on the fibers will be nearly equivalent. This implies that the weight sensitivity of the fiber is about 0.0035 nm per pg/mm^2. Accounting for the molecular weight of streptavidin 2.43 ± 0.54 pmol of protein is bound per 1 cm^2 surface.

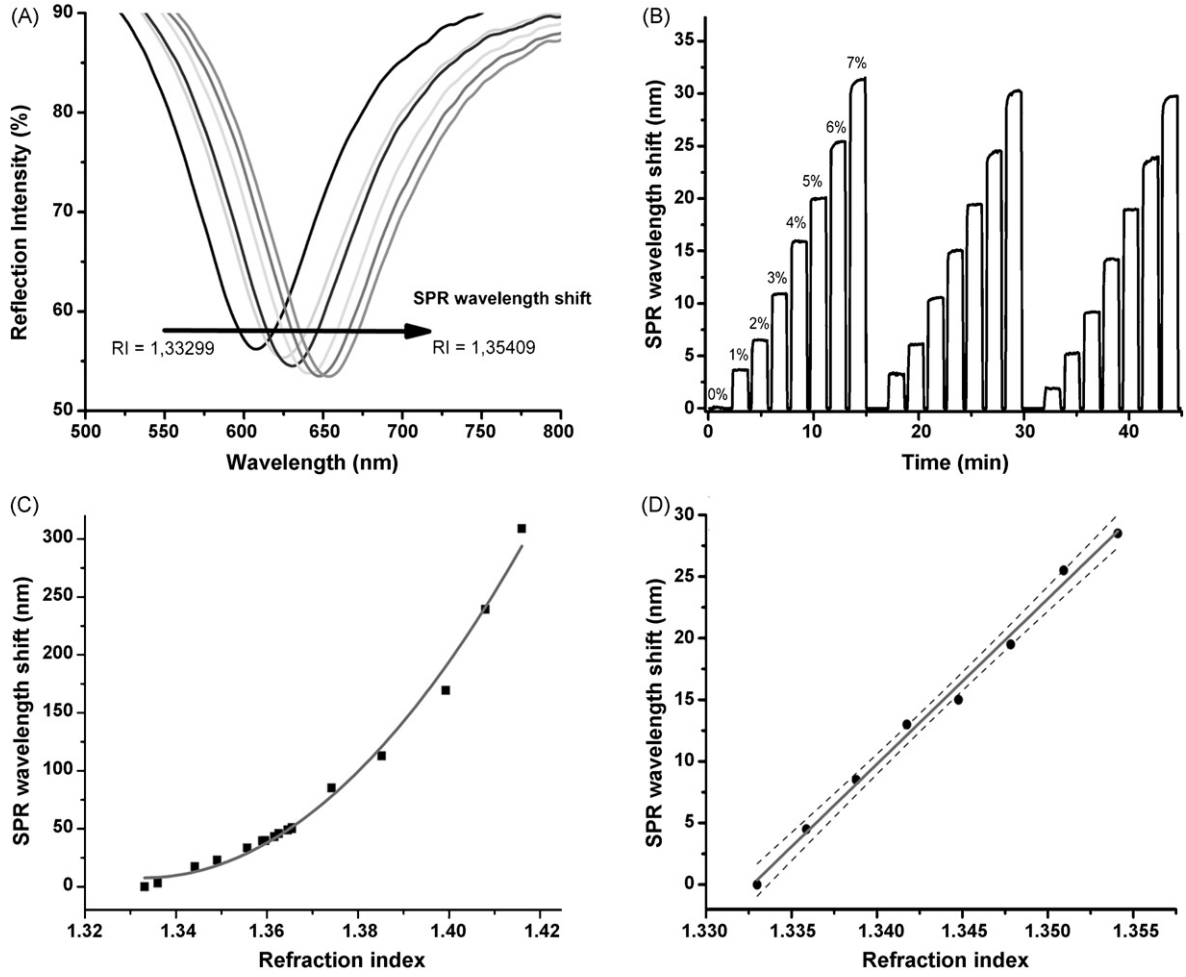

Fig. 2. Fiber calibration results. (A) Intensity dips of the reflected light due to the resonance effect. A higher refraction index (RI) forces the spectra to shift to the longer wavelengths. (B) A time resolved graph of three consecutive repetitions of a set of sucrose solutions containing 1–7% sucrose. (C) Calibration curve for a wide range of refraction indices based on different alcohol–water mixtures. (D) Linear calibration curve for refraction index based on water–ethanol dilutions.

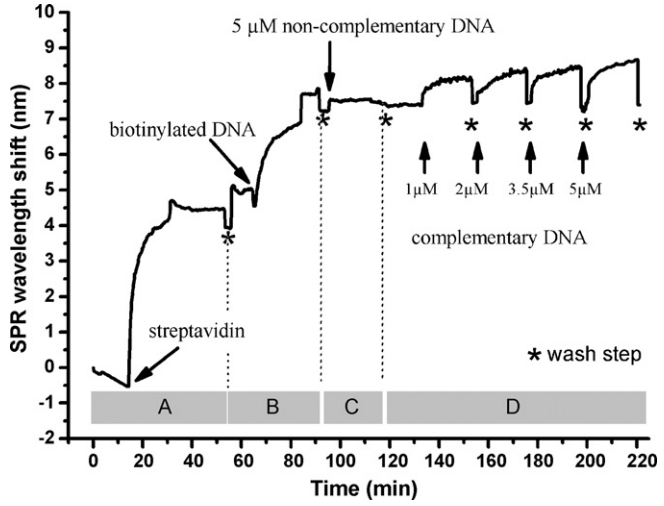

Fig. 3. Sensorgram of hybridization experiment. (Block A) Streptavidin immobilization in MES buffer. (Block B) Binding of biotinylated receptor DNA in TRIS buffer. (Block C) Hybridization of 5 μM non-complementary DNA in 1 M NaCl TRIS buffer. (Block D) Hybridization of different concentrations of complementary DNA ranging 1–5 μM in 1 M NaCl TRIS buffer.

In a next step, biotinylated ssDNA was attached to the immobilized streptavidin (Figs. 3 and 5, Block B). Afterwards the fiber sensor surface was washed again with NaOH (50 mM) in NaCl (1 M) to remove any free DNA. As expected, the observed wavelength shift depends on the molecular weight. The latter is illustrated by comparing Block B of Fig. 3 with Block B of Fig. 5. The SPR wavelength shift caused by the biotinylated 63-mer extended aptamer (18.9 kDa) is 5.0 ± 1.0 nm, this is about 2.5 times higher than the 2.1 ± 1.0 nm shift induced by the biotinylated 25-mer DNA probe (7.9 kDa) used in the hybridization assay. Based on the molecular weight and the weight related sensitivity number, an immobilization density of 7.34 ± 1.47 pmol/cm^2 was calculated for the aptamer and 7.36 ± 3.51 pmol/cm^2 for the DNA probe. In other words 3.01 biotinylated DNA strands are captured per streptavidin. In an identical experiment on the Biacore 3000 this number was confirmed.

3.3. DNA hybridization assay

The potential of the ssDNA functionalized SPR probes was evaluated as a nucleic acid biosensor through a hybridization assay, similar to the experiments of Wang et al. (2004) on the Biacore 3000 platform. A streptavidin coated fiber was incubated for 15 min with 0.5 μM of a 25-mer biotinylated ssDNA strand in 100 μl TRIS buffer. The corresponding signal is shown in Fig. 3 Blocks A and B. Next, the fiber was used to measure hybridization with a 37-mer ssDNA which had a 15 nucleotides long overlap with the receptor ssDNA on

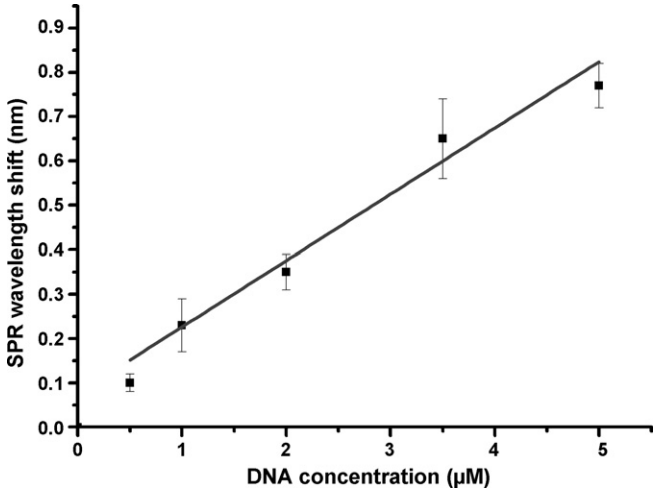

Fig. 4. Calibration curve of hybridization experiment.

the SPR fiber (Fig. 3 Block C). After 15 min binding equilibrium was reached. A linear correlation was observed for a calibration curve performed in a 0.5–5 μM range (Fig. 4). A negative control experiment was carried out with a 37-mer non-complementary ssDNA strand (Fig. 3 Block D) to test specificity and to validate the repulsion efficiency of the PEG-based coating at the sensor probe surface with respect to non-specific ssDNA binding. After each assay the sensor was regenerated with a short acid treatment (1.25 mM HCl) to denature the DNA. After a few measurement cycles only a slight downward drift of the resonance baseline was noticed, implying limited release of the immobilized ssDNA primer. Nevertheless, the DNA coated fibers could be regenerated for at least 20 times without a significant change in sensing performance. Other researchers who tested the stability of the DNA on gold layers concluded that the layer was stable even after 100 regenerations (Wang et al., 2004).

3.4. hIgE Aptamer assay

In a second assay ssDNA aptamers against hIgE were immobilized onto the SPR probe to quantify hIgE. Block C of Fig. 5A shows the association phase for six different concentrations of hIgE ranging from 10 up to 500 nM. For hIgE concentrations lower than 200 nM, the binding equilibrium between the immobilized aptamers and the target proteins only reaches full equilibrium after 15 min. Full equilibrium is however not mandatory for quantification, and hence, the SPR signal after 4 min was measured in order to speed up the assay, without a significant loss in sensor performance characteristics. Since the amount of aptamers that can be immobilized at the surface is limited, the sensor signal saturates when the amount of hIgE is abundant, resulting in a non-linear (Fig. 5B) calibration curve. However, for a detection limit up to 100 nM, a linear response was observed (Fig. 5C). The SPR sensor limit of detection was estimated to be 2 ± 1 nM (~0.5 μg/ml) based on a signal to noise ratio of 3. The limit of quantification was taken as three times the limit of detection and equals 6 ± 2 nM. Compared to the DNA assay, the sensor has a lower detection limit for the protein, since the SPR phenomenon is more sensitive towards higher molecular weight molecules: the binding of one hIgE molecule to the surface results in a larger refractive index shift than the binding of a 37-mer DNA strand. No significant resonance shift was visible in the sensorgram when the same experiment was repeated with hIgG, confirming the specificity and the repulsive character of the PEG layer. By changing the amount of aptamers immobilized on the sensor surface, the sensor sensitivity or detection range might further be improved.

The SPR sensorgrams of the biosensor also reveal the binding kinetics occurring at the sensor surface. As a reference, the binding kinetics of aptamer with hIgE were evaluated using laser induced fluorescence affinity capillary electrophoresis (ACE) based on the protocols as described by Berezovski et al. (2006), and on the Biacore 3000. A dissociation constant (K_D) of 52 ± 10 nM was calculated through ACE. On a Biacore 3000, the hIgE affinity towards the aptamer was found to be slightly better with a $K_D = 20 \pm 2$ nM. The difference could be explained by steric hindrance caused by the fluorescent FAM label used in the ACE method. (German et al., 1998). To determine the binding kinetics on the fiber, SPR curves for different concentrations of hIgE were fitted with a global 1:1 Langmuir-based association/dissociation model. The measured and the modeled kinetic data show a high correspondence as is illustrated in Fig. 6. The SPR fiber estimated the association rate constant, $k_{on} = 6.94 \times 10^4 \pm 0.21 \times 10^4\ M^{-1}\ s^{-1}$ and the dissociation rate constant, $k_{off} = 2.14 \times 10^{-3} \pm 0.19 \times 10^{-3}\ s^{-1}$, and hence a K_D of $3.09 \times 10^{-8} \pm 0.29 \times 10^{-8}$ M, confirming the results of the affinity study on capillary electrophoresis and the Biacore 3000. Our general kinetic data on hIgE aptamers can be aligned with the data published by Wang et al. (2008) but not with the recent paper of Kim et al. (2009) where they reported a very slow dissociation ($k_{off} = 2.21 \times 10^{-6}\ s^{-1}$), and suggested a $K_D = 2.30 \times 10^{-11}$ M.

The maximum response, R_{max}, was 2.71 ± 0.06 nm or in other words, 0.387 pmol of hIgE protein was bound per cm^2. Conse-

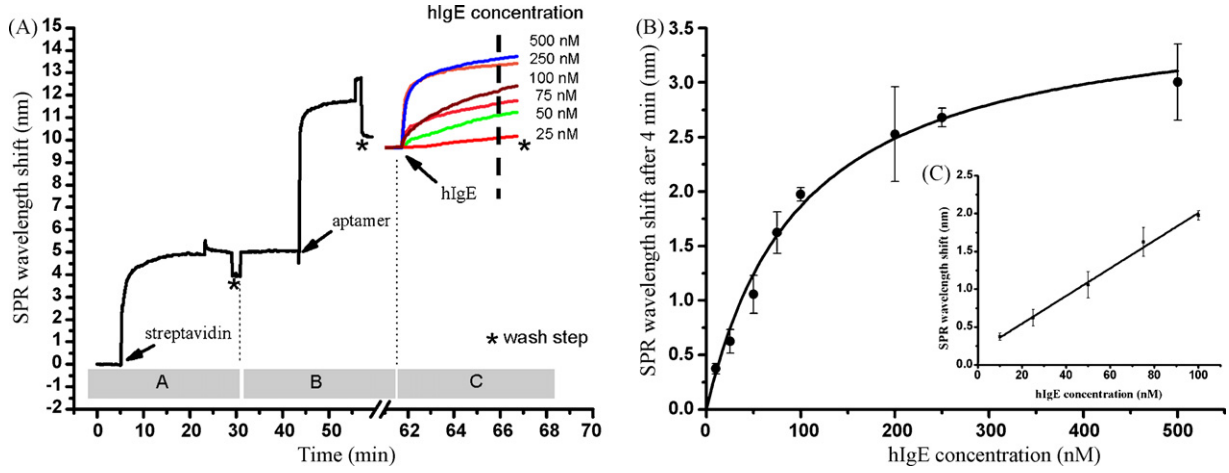

Fig. 5. Aptamer-based hIgE protein detection experiment. (A) Sensorgram: (Block A) Streptavidin immobilization in MES buffer. (Block B) Binding of biotinylated DNA in TRIS buffer. (Block C) Kinetic data of hIgE binding to the aptamer in TGK buffer. (B) Non-linear hIgE calibration curve after 4 min. (C) Linear hIgE calibration curve after 4 min.

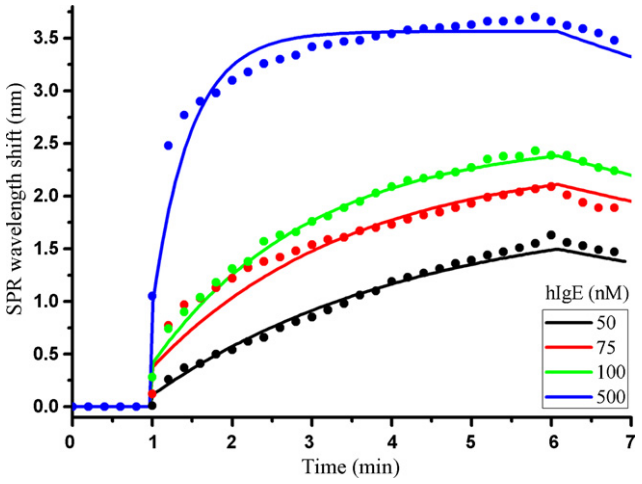

Fig. 6. Global association/dissociation analysis of the kinetic data for hIgE.

quently, only one in 18 aptamers captures a hIgE molecule and there is only one immunoglobulin per 6 streptavidin molecules. This is due to large size of hIgE. If one of the DNA strands on the streptavidin captures a hIgE molecule then the other DNA strands attached to the same streptavidin molecule will most likely be unable to bind a second one due to steric hindrance. This effect might even play for neighboring DNA–streptavidin supramolecular structures. Taking an effective diameter of hIgE (190 kDa) of 11 nm, the same as that of IgG (150 kDa), we estimated that one IgE molecule occupies a surface area of 100 nm^2 (Ding et al., 2009) and calculated that for 500 nM protein, when the signal of the hIGE sensor saturates, approximately 25% of the sensor surface was covered with hIgE.

4. Conclusion

Small fiber-based SPR probes were produced in the lab and integrated in a fully automated setup. Mainly by using a tungsten white light source and removing the need for microfluidics, the system is approximately 2 factors less expensive than most commercially available SPR platforms. It has been shown that these fiber optic biosensors are not only useful for the quantification of DNA or proteins in a biological sample, but also to monitor the association and the dissociation of biomolecular interactions in real-time. Two biosensing assays employing DNA bioreceptors were evaluated in this paper. First biotinylated ssDNA was immobilized on streptavidin coated SPR probes to detect complementary ssDNA in the concentration range from 0.5 to 5 μM. Non-complementary DNA induced no significant SPR resonance shift. This assay can be used to quantify short DNA fragments after PCR amplification. Second, based on the same surface chemistry, ssDNA aptamers against hIgE were attached to the biosensor probe. With the fiber optic SPR sensor it was possible to detect hIgE in the low nanomolar range (2 nM), while quantification was possible in the concentration range from 6 to 100 nM.

It was further illustrated that the sensors are very useful to evaluate the binding kinetics of the aptamer bioreceptor to the immunoglobulin protein. The SPR sensor revealed a dissociation constant of 30.9 ± 2.9 nM, which perfectly matches the values reported by others and our own verification experiments. The fiber optic sensors could easily be regenerated and were used for multiple testing. Human serum spiked hIgE will be used in additional experiments as an example for measuring in more complex matrices. The results illustrate that by combining the small, low cost SPR sensors with good surface chemistry very sensitive and cost-effective nucleic acid biosensors are developed.

This low cost will make the presented technology more accessible for many applications. In the near future we will exploit this system further as a screening tool for diverse protein–protein and protein–DNA interactions for medical diagnostics, environmental diagnostics and, food quality and safety applications.

Acknowledgements

The authors are grateful to the 'Instituut voor aanmoediging van innovatie door Wetenschap en Technologie' (IWT 63384), Fund for Scientific Research Flanders (FWO G.0298.06 and FWO G.0603.08), and the Industrial Research Fund K.U. Leuven (IOF) for their financial support.

References

Berezovski, M.V., Musheev, M.U., Drabovich, A.P., Jitkova, J.V., Krylov, S.N., 2006. Nat. Protoc. 1, 1359–1369.
Buchanan, D.D., Jameson, E.E., Perlette, J., Malik, A., Kennedy, R.T., 2003. Electrophoresis 24, 1375–1382.
de-los-Santos-Alvarez, N., Lobo-Castanon, M.J., Miranda-Ordieres, A.J., Tunon-Blanco, P., 2008. Trends Anal. Chem. 27, 437–446.
Ding, S., Gao, C., Gu, L.Q., 2009. Anal. Chem. 81, 6649–6655.
German, I., Buchanan, D.D., Kennedy, R.T., 1998. Anal. Chem. 70, 4540–4545.
Gong, M., Wehmeyer, K.R., Limbach, P.A., Heineman, W.R., 2007. Electrophoresis 28, 837–842.
Grunwald, B., Holst, G., 2004. Sens. Actuators A 113, 174–180.
Homola, J., Piliarik, M., 2006. Surface Plasmon Resonance (SPR) Sensors. In: Homola, J. (Ed.), Surface plasmon resonance based sensors. Springer, Berlin Heidelberg, pp. 45–67.
Jans, K., Bonroy, K., De, P.R., Reekmans, G., Jans, H., Laureyn, W., Smet, M., Borghs, G., Maes, G., 2008. Langmuir 24, 3949–3954.
Jayasena, S.D., 1999. Clin. Chem. 45, 1628–1650.
Jorgenson, R.C., Yee, S.S., 1993. Sens. Actuators B 12, 213–220.
Kim, Y.H., Kim, J.P., Han, S.J., Sim, S.J., 2009. Sens. Actuators B 139, 471–475.
Masson, J.F., Kim, Y.C., Obando, L.A., Peng, W., Booksh, K.S., 2006. Appl. Spectrosc. 60, 1241–1246.
Mayer, G., 2009. Angew. Chem. Int. Ed. 48, 2672–2689.
Mitsushio, M., Higo, M., 2004. Anal. Sci. 20, 689–694.
Myszka, D.G., 1999. J. Mol. Recognit. 12, 279–284.
Obando, L.L., Booksh, K.S., 1999. Anal. Chem. 71, 5116–5122.
Palegrosdemange, C., Simon, E.S., Prime, K.L., Whitesides, G.M., 1991. J. Am. Chem. Soc. 113, 12–20.
Shankaran, D.R., Miura, N., 2007. J. Phys. D: Appl. Phys. 40, 7187–7200.
Slavik, R., Homola, J., Ctyroky, J., 1999. Sens. Actuators B 54, 74–79.
Song, S.P., Wang, L.H., Li, J., Zhao, J.L., Fan, C.H., 2008. Trends Anal. Chem. 27, 108–117.
Wang, J.L., Lv, R.J., Xu, J.J., Xu, D.K., Chen, H.Y., 2008. Anal. Bioanal. Chem. 390, 1059–1065.
Wang, R.H., Minunni, M., Tombelli, S., Mascini, M., 2004. Biosens. Bioelectron. 20, 598–605.
Wiegand, T.W., Williams, P.B., Dreskin, S.C., Jouvin, M.H., Kinet, J.P., Tasset, D., 1996. J. Immunol. 157, 221–230.
Yang, N., Su, X.D., Tjong, V., Knoll, W., 2007. Biosens. Bioelectron. 22, 2700–2706.